

# Phase diagram of the (bosonic) Double-Exchange Model

J. L. Alonso,<sup>1,2</sup> A. Cruz,<sup>1,2</sup> L. A. Fernández,<sup>3,2</sup> S. Jiménez,<sup>1,2</sup>  
V. Martín-Mayor,<sup>3,2</sup> J. J. Ruiz-Lorenzo,<sup>4,2</sup> and A. Tarancón<sup>1,2</sup>

<sup>1</sup>*Departamento de Física Teórica, Facultad de Ciencias,  
Universidad de Zaragoza, 50009 Zaragoza, SPAIN*

<sup>2</sup>*Instituto de Biocomputación y Física de Sistemas Complejos (BIFI)*

<sup>3</sup>*Departamento de Física Teórica, Facultad de Ciencias Físicas,  
Universidad Complutense, 28040 Madrid, SPAIN*

<sup>4</sup>*Departamento de Física, Facultad de Ciencias,  
Universidad de Extremadura, 06071 Badajoz, SPAIN*

(Dated: November 7, 2018)

The phase diagram of the simplest approximation to Double-Exchange systems, the bosonic Double-Exchange model with antiferromagnetic super-exchange coupling, is fully worked out by means of Monte Carlo simulations, large- $N$  expansions and Variational Mean-Field calculations. We find a rich phase diagram, with no first-order phase transitions. The most surprising finding is the existence of a segment like ordered phase at low temperature for intermediate AFM coupling which *cannot be detected in neutron-scattering experiments*. This is signaled by a maximum (a cusp) in the specific heat. Below the phase-transition, only short-range ordering would be found in neutron-scattering. Researchers looking for a Quantum Critical Point in manganites should be wary of this possibility. Finite-Size Scaling estimates of critical exponents are presented, although large scaling corrections are present in the reachable lattice sizes.

PACS numbers: 75.30.Et, 64.60.Fr, 05.10.Ln.

## I. INTRODUCTION

There are at least two motivations for studying the spin-only version of the Double-Exchange (DE) models. On the one hand one, has its relationship with the Colossal Magnetoresistance effect (CMR).<sup>1,2,3</sup> On the other hand, in this problem some puzzles arise<sup>4</sup> with the Universality Hypothesis,<sup>5</sup> that deserve a detailed study. Let us start addressing the first aspect.

CMR has renewed the interest in Double-Exchange (DE) systems.<sup>6</sup> The typical CMR manganites are  $\text{La}_{1-x}\text{AE}_x\text{Mn}_{1-y}\text{O}_3$ , where  $\text{AE}=\text{Ca}, \text{Sr}$  in the range  $0.2 < x < 0.5$ . It is believed that the relevant degrees of freedom<sup>1</sup> are the localized  $S = 3/2$   $\text{Mn}^{3+}$  core spins, and the  $\text{e}_g$  holes. The  $\text{Mn}^{3+}$  ions form a single cubic lattice and, besides the DE mechanism, interact through an antiferromagnetic (AFM) superexchange coupling. The relatively high spin of the  $\text{Mn}^{3+}$  core suggests to treat them as classical spins,  $\vec{\phi}_i$ . Although phonons are believed to be crucial for the CMR effect,<sup>7</sup> manganites display a very rich magnetic phase diagram which can be addressed neglecting lattice effects.<sup>8</sup> In spite of these simplifications, and of the introduction of powerful new tools,<sup>9,10,11</sup> the numerical study of the DE model in large lattices beyond Mean Field Approximation is out of reach for present day computers. Yet, finite-size effects in these systems are unusually large.<sup>8</sup> The need to obtain reliable predictions has made people to further simplify models, replacing  $\text{e}_g$  holes by an effective interaction among the localized  $S = 3/2$   $\text{Mn}^{3+}$  core spins. Indeed, a simple calculation<sup>6</sup> shows that the kinetic energy of the electrons depends on the relative orientation of neighboring

$\text{Mn}^{3+}$  core spins as  $\sqrt{1 + \vec{\phi}_i \cdot \vec{\phi}_j}$ . This substitution of a simpler spin-only problem in place of the very difficult electronic problem lies at the heart of several theoretical analyses (see e.g. de Gennes in Ref. 6) and numerical simulations.<sup>12</sup> In spite of this, up to our knowledge there is only one detailed previous study<sup>13</sup> of the phase-diagram of the bosonic DE model. That study predicted the existence of a disordered (PM) phase at very low temperatures for intermediate super-exchange coupling. This is very reminiscent of the presence of a Quantum-Critical Point<sup>14</sup> which is believed to be of importance for the CMR phenomenon,<sup>15</sup> and has been predicted to occur in manganites by some model calculations.<sup>16</sup> The experimental characterization of this Quantum Critical Point is a wedge of paramagnetic (PM) phase, maybe glassy,<sup>17</sup> that at zero temperature becomes a single point separating two ordered phases.<sup>15</sup> The glassy wedge would be created by disorder,<sup>15</sup> and would be separated from the Paramagnetic state at high-temperature scale  $T^*$ . Maybe the most surprising result of the here presented analysis is that this glassy wedge could not be PM or glassy at all, but ordered in a segment-like way<sup>18,19,20</sup> (as in liquid crystals). This ordering will be referred to in the following as  $\text{RP}^2$  (real projective space). As we shall show, the  $\text{RP}^2$  phase cannot be detected in neutron-scattering experiments (although a short-range ordering will be present). Nevertheless, the phase-transition can be studied experimentally using the specific-heat, that should present a maximum (furthermore, a cusp) at the critical temperature. Indeed, the thermal critical exponent is predicted<sup>4</sup> to be  $\nu = 0.78(2)$  which implies  $\alpha = -0.34$ , and hence the cusp behavior follows. Another bonus of our simplified model is that it allows us

to study qualitatively (see subsection IV C) the funny interplay between ferromagnetism, antiferromagnetism, temperature and applied magnetic field in low-doped  $\text{La}_{1-x}\text{Sr}_x\text{MnO}_3$ .<sup>21,22,23,24</sup>

Let us now address Universality. A common wisdom is that the critical properties of a system are given by its dimensionality and the local properties (i.e. near the identity element) of the coset space  $\mathcal{G}/\mathcal{H}$ , where  $\mathcal{G}$  is the symmetry group of the Hamiltonian (the symmetry of the high temperature phase) and  $\mathcal{H}$  is the remaining symmetry group of the broken phase (low temperature). So, systems with locally isomorphic  $\mathcal{G}/\mathcal{H}$  belong to the same Universality Class. This seems to be true in perturbation theory, where the observables are computed by doing series expansions around the identity element of  $\mathcal{G}/\mathcal{H}$ . In this picture, a phase transition of a vector model, with  $O(3)$  global symmetry and with an  $O(2)$  low temperature phase symmetry, in three dimensions must belong to the  $O(3)/O(2)$  scheme of symmetry breaking (classical Heisenberg model). In addition, if  $\mathcal{H}=O(1)=Z_2$  is the remaining symmetry, the corresponding scheme should be<sup>25</sup>  $O(4)/O(3)$  which is locally isomorphic to  $O(3)/O(1)$ .

Hence, it is interesting to check if the global properties of the coset space  $\mathcal{G}/\mathcal{H}$  are relevant or not to the phase transition. The common wisdom has been challenged in the past by the so-called chiral models.<sup>26</sup> However, the situation is still hotly debated: some authors believe that the chiral transitions are weakly first-order,<sup>27</sup> while others claim<sup>28</sup> that the Chiral Universality Class exists, implying the relevance of the global properties of  $\mathcal{G}/\mathcal{H}$ . On the other hand, we do not have any doubt about the second order nature of the PM-RP<sup>2</sup> transition. A detailed study of the critical exponents was recently published<sup>4</sup> in Letter form. In the present work, we perform a detailed Monte Carlo, Mean Field and large- $N$  study of the phase diagram. A thorough study is performed of the RP<sup>2</sup> phase. We shall confirm that the pattern of symmetry breaking is  $O(3)/O(2)$ , implying a violation of Universality for which we do not have any plausible explanation.

The layout of the rest of this paper is as follows. In section II we define the model, study the phase diagram at zero temperature, and define the order parameters and observables measured in the Monte Carlo simulations. The Mean-Field calculation is explained in section III, where we also report the results of the Large- $N$  analysis. In section IV we present our Monte Carlo results. We start determining the global phase diagram in subsection IV A. The RP<sup>2</sup> phase is investigated in more detail in subsection IV B, while the effects of a magnetic field on conductivity close to a ferromagnetic-antiferromagnetic transition is considered in subsection IV C. We present our conclusions in section V. We complement the paper with two appendices. Appendix A contains the details about the large- $N$  calculation. In Appendix B the reader will find the Mean-Field phase diagram as obtained from the fourth-order expansion of the Free-Energy.

## II. THE MODEL

### A. The Hamiltonian

We define a system of spins  $\{\vec{\phi}_i\}$  living in a three dimensional cubic lattice of size  $L$  (and volume  $V = L^3$ ) with periodic boundary conditions. The spins are three-component real unit vectors. We consider the Hamiltonian

$$H = - \sum_{\langle i,j \rangle} \left( J \vec{\phi}_i \cdot \vec{\phi}_j + \sqrt{1 + \vec{\phi}_i \cdot \vec{\phi}_j} \right), \quad (1)$$

where the sum is extended to all pairs of nearest neighbors and we consider only  $J < 0$ . Notice that we will measure temperature in units of the double exchange constant. The cubic lattice is bipartite, therefore we shall call the lattice site  $i$  *even* or *odd* according to the parity of the sum of its coordinates,  $x_i + y_i + z_i$ .

We will consider the system at a temperature  $T$ , the partition function being

$$Z = \int \prod_i d\vec{\phi} e^{-H/T}, \quad (2)$$

where the integration measure is the standard measure on the unit sphere.

### B. Phase diagram at zero temperature

As usual, the study of the phase diagram begins with an understanding of the ordered phases at zero temperature. We can write in a compact way our original Hamiltonian:

$$H = - \sum_{\langle i,j \rangle} \mathcal{V}(\vec{\phi}_i \cdot \vec{\phi}_j), \quad (3)$$

where

$$\mathcal{V}(y) = Jy + \sqrt{1+y^2}, \quad (4)$$

and clearly  $y \in [-1, 1]$ . In the limit of zero temperature, the only configurations which contribute to the partition function are those which provide a maximum of  $\mathcal{V}(y)$ . If, as confirmed by the Monte Carlo simulations, the spin texture itself is bipartite, the value of  $y$  will be uniform through the lattice. Thus, a simple computation yields that the maxima of  $\mathcal{V}(y)$  are at the following values of  $y$  (denoted by  $y_{\max}$ )

$$y_{\max} = \begin{cases} 1 & \text{for } J \geq -\frac{1}{2\sqrt{2}} \\ -1 + \frac{1}{4J^2} & \text{for } J \leq -\frac{1}{2\sqrt{2}}. \end{cases} \quad (5)$$

It is clear that  $y_{\max} = 1$  corresponds to a ferromagnetic state and that in the  $J \rightarrow -\infty$  limit we reach an antiferromagnetic one ( $y_{\max} = -1$ ). The intermediate values

of  $y_{\max}$  correspond to a ferrimagnet if  $0 < y_{\max} < 1$  and to an anti-ferrimagnet when  $-1 < y_{\max} < 0$ . The physical picture is as follows: the spins in the, say, even sublattice are all parallel along (for instance) the Z-axis. On the other hand the odd spins lie on a cone forming an angle  $\theta$  ( $\cos \theta = y_{\max}$ ) with the Z-axis.

The corresponding free energy is just

$$f(J) = \begin{cases} \sqrt{2} + J & \text{for } J \geq -\frac{1}{2\sqrt{2}}, \\ -\frac{1}{4J} - J & \text{for } J \leq -\frac{1}{2\sqrt{2}}. \end{cases} \quad (6)$$

Hence we have the following phase transitions:

1. Ferromagnetic-ferrimagnetic at  $J = -1/\sqrt{8}$ . It is easy to check that  $df/dJ$  is continuous at  $J = -1/\sqrt{8}$  but  $d^2f/dJ^2$  is discontinuous. Hence, according to the standard Erhenfest classification, we have a second order phase transition.
2. Ferrimagnetic-antiferrimagnetic at  $J = -1/2$ , where the free-energy is  $C^\infty$ . At this special point  $y_{\max}$  changes from positive to negative. The fact that  $y_{\max} = 0$  implies that one can reverse every single spin independently of the others without changing the energy (more pedantically, one finds a dynamically generated  $Z_2$  gauge symmetry<sup>4</sup>).
3. The limiting value  $y_{\max} = -1$  that corresponds to an antiferromagnet rather than an antiferrimagnet is reached only at  $J = -\infty$ .

The transition 2 (Ferrimagnet-antiferrimagnet) needs further discussion. We can expand the Hamiltonian around the minimum  $y = 0$ , and we obtain

$$\mathcal{V}(y) = 1 - \frac{1}{8}y^2 + \mathcal{O}(y^3). \quad (7)$$

Thus, close to  $J = -0.5$  and  $T = 0$  one has, neglecting constant terms,

$$H = \frac{1}{8} \sum_{\langle i,j \rangle} (\vec{\phi}_i \cdot \vec{\phi}_j)^2 + \mathcal{O}\left((\vec{\phi}_i \cdot \vec{\phi}_j)^3\right), \quad (8)$$

which corresponds to an *anti*-ferromagnetic  $RP^2$ -theory. The minimum energy configuration satisfies  $y = 0$ . Hence, we obtain that the ferrimagnet-antiferrimagnet transition occurs at zero temperature via a  $RP^2$  state at a single point. We shall see that at finite temperature the  $RP^2$  phase occupies a region (rather than a single point) of the phase diagram.

From the previous analysis at zero temperature, one expects to find the following phases at finite temperature:

- PM: the usual disordered state, where all the symmetries of the model are preserved.
- FM: a standard ferromagnetic ordering, i.e., the spin fluctuates around  $(0, 0, 1)$ .

- AFM: a standard anti-ferromagnetic ordering. Even (odd) spins fluctuate around  $\vec{\phi}^e = (0, 0, 1)$  ( $\vec{\phi}^o = (0, 0, -1)$ ).
- FI: The ordering consists on even spins fluctuating around the Z axis and odd spins fluctuating around the cone of angle  $\theta < \pi/2$  with axis Z.
- AFI: This ordering is similar to the previous one, with  $\theta > \pi/2$ .
- $RP^2$ : Here the ordering is the finite  $T$  version of the one found analytically in  $J = -0.5, T = 0$ , i.e., even spins fluctuating around the Z axis, with random sense, and odd spins fluctuating around the cone with random sense.

### C. Order Parameters

In models with antiferromagnetic couplings, one might expect an even-odd structure of the ordered phases. Therefore, from the local field  $\{\vec{\phi}_i\}$ , we define the standard magnetization as the Fourier transform at momentum 0, and the staggered magnetization as the Fourier transform at momentum  $(\pi, \pi, \pi)$ :

$$\vec{M} = \frac{1}{L^3} \sum_i \vec{\phi}_i, \quad (9)$$

$$\vec{M}_s = \frac{1}{L^3} \sum_i (-1)^{x_i+y_i+z_i} \vec{\phi}_i. \quad (10)$$

In a finite lattice we must take the modulus before taking the mean value. We will study:

$$\mu^V = \langle \|\vec{M}\| \rangle, \quad (11)$$

$$\mu_s^V = \langle \|\vec{M}_s\| \rangle. \quad (12)$$

The associated susceptibilities are

$$\chi^V = L^3 \langle \vec{M}^2 \rangle, \quad (13)$$

$$\chi_s^V = L^3 \langle \vec{M}_s^2 \rangle. \quad (14)$$

In order to explore  $RP^2$  type phases we introduce the tensor invariant under the local spin reversal. In this case we use as local field the matrices  $\{\tau_i\}$ , constructed as

$$\tau_i = \phi_i^\alpha \phi_i^\beta - \frac{1}{3} \delta^{\alpha\beta}; \quad \alpha, \beta = 1, 2, 3. \quad (15)$$

Notice that they are traceless, thus they represent objects of spin 2. We can now define the associated traceless tensor magnetizations

$$M = \frac{1}{L^3} \sum_i \tau_i, \quad (16)$$

$$M_s = \frac{1}{L^3} \sum_i (-1)^{x_i+y_i+z_i} \tau_i, \quad (17)$$

and the mean values:

$$\mu^T = \langle \sqrt{\text{Tr } M^2} \rangle, \quad (18)$$

$$\mu_s^T = \langle \sqrt{\text{Tr } M_s^2} \rangle. \quad (19)$$

The corresponding susceptibilities are

$$\chi^T = L^3 \langle \text{Tr } M^2 \rangle, \quad (20)$$

$$\chi_s^T = L^3 \langle \text{Tr } M_s^2 \rangle. \quad (21)$$

Let us close this subsection recalling the value of the order parameters (in the large volume limit) in each of the ordered phases found in the previous subsection:

$$\begin{aligned} \text{FM: } & \mu^V > 0, \mu_s^V = 0 \quad (\Rightarrow \mu^T > 0, \mu_s^T = 0), \\ \text{AFM: } & \mu_s^V > 0, \mu^V = 0 \quad (\Rightarrow \mu^T > 0, \mu_s^T = 0), \\ \text{FI: } & \mu^V > \mu_s^V > 0 \quad (\Rightarrow \mu^T, \mu_s^T > 0), \\ \text{AFI: } & \mu_s^V > \mu^V > 0 \quad (\Rightarrow \mu^T, \mu_s^T > 0), \\ \text{RP}^2: & \mu_s^T > \mu^T > 0, \mu_s^V = \mu^V = 0. \end{aligned} \quad (22)$$

#### D. Correlation Length

For an antiferromagnetic model, not only the usual susceptibility, also the staggered susceptibility can diverge. Thus, in the Brillouin zone, one needs to monitor the behavior of the Green functions close to the origin as well as close to  $(\pi, \pi, \pi)$ . Since in critical-phenomena studies one usually considers only the behavior around zero momentum, we have found it convenient to define four Green functions in terms of four fields in momentum space

$$\hat{\phi}(\mathbf{p}) = \sum_i e^{-i\mathbf{p} \cdot \mathbf{r}_i} \vec{\phi}_i, \quad (23)$$

$$\hat{\phi}_s(\mathbf{p}) = \sum_i e^{-i\mathbf{p} \cdot \mathbf{r}_i} (-1)^{x_i+y_i+z_i} \vec{\phi}_i, \quad (24)$$

$$\hat{\tau}(\mathbf{p}) = \sum_i e^{-i\mathbf{p} \cdot \mathbf{r}_i} \tau_i, \quad (25)$$

$$\hat{\tau}_s(\mathbf{p}) = \sum_i e^{-i\mathbf{p} \cdot \mathbf{r}_i} (-1)^{x_i+y_i+z_i} \tau_i, \quad (26)$$

the Fourier transforms of the correlation functions being

$$\hat{G}^V(\mathbf{p}) = \frac{1}{L^3} \langle \hat{\phi}(\mathbf{p}) \cdot \hat{\phi}^*(\mathbf{p}) \rangle, \quad (27)$$

$$\hat{G}_s^V(\mathbf{p}) = \frac{1}{L^3} \langle \hat{\phi}_s(\mathbf{p}) \cdot \hat{\phi}_s^*(\mathbf{p}) \rangle, \quad (28)$$

$$\hat{G}^T(\mathbf{p}) = \frac{1}{L^3} \langle \text{Tr } \hat{\tau}(\mathbf{p}) \hat{\tau}^\dagger(\mathbf{p}) \rangle, \quad (29)$$

$$\hat{G}_s^T(\mathbf{p}) = \frac{1}{L^3} \langle \text{Tr } \hat{\tau}_s(\mathbf{p}) \hat{\tau}_s^\dagger(\mathbf{p}) \rangle. \quad (30)$$

Notice that  $\hat{G}_s^{V,T}(\mathbf{p}) = \hat{G}^{V,T}(\mathbf{p} + (\pi, \pi, \pi))$ , so that one could consider only non staggered correlation functions that would be studied both close to  $(0, 0, 0)$  and to  $(\pi, \pi, \pi)$ .

Near a (continuous) phase transition where the corresponding correlation length,  $\xi$ , diverges, the correlation functions in the thermodynamic limit behave for small  $\mathbf{p}^2 \xi^2$ , as

$$\hat{G}(\mathbf{p}) \simeq \frac{Z \xi^{-\eta}}{\mathbf{p}^2 + \xi^{-2}}. \quad (31)$$

Here  $\xi$  diverges as  $|t|^{-\nu}$ ,  $t$  being the reduced temperature. The anomalous dimension,  $\eta$ , will depend on the considered field.

In a finite lattice, to estimate the correlation length one uses the propagator at zero momentum and at the minimum non-zero momentum compatible with boundary conditions. Defining  $F = \hat{G}(2\pi/L, 0, 0)$  and noting that  $\chi = \hat{G}(0)$ , one has<sup>29</sup>

$$\xi = \left( \frac{\chi/F - 1}{4 \sin^2(\pi/L)} \right)^{1/2}. \quad (32)$$

### III. MEAN FIELD CALCULATION

When several phases compete, it is quite tricky to calculate the phase diagram in Mean-Field approximation (the  $T = 0$  calculation has shown that we should face this problem!). Since one can find different ordered phases at low temperatures within different Mean-Field schemes, it is necessary to decide which phase shall be the most stable one. We consider that the cleanest way of performing such a calculation is to use the variational formulation of the Mean-Field approximation (see for example Ref. 30), with a variational family large enough to take into account all the phases found in the phase diagram. In this way, all the phases compete on the same grounds and one has an objective criterion to decide which phase is to be found in a given region of the phase-diagram.

One needs to compare the actual system with a simplified model where all degrees of freedom are statistically independent. The method is derived from the inequality<sup>30</sup>

$$F \leq F_0 + \langle H - H_0 \rangle_0. \quad (33)$$

Here,  $H_0$  is a trial Hamiltonian depending on some parameters (the *mean fields*) and the average  $\langle \dots \rangle_0$  means average with the Boltzmann weight corresponding to  $H_0$ . The right-hand side of the inequality (33) is minimized with respect to the free parameters in  $H_0$ , then used as our best estimate of the Free-energy. Thus the task is to generalize the standard Curie-Weiss ansatz,  $H_0 = h \sum_i \phi_i^z$ , ( $\phi_i^z$  is the component of the local spin  $\vec{\phi}_i$  along the Z-axis), to cover all the expected orderings.

In our case, we must use the simplest possible variational family that permits to have different orderings in the even and odd sublattices:

$$H_0 = - \sum_{i \text{ even}} V_e(\phi_i^z) - \sum_{i \text{ odd}} V_o(\phi_i^z). \quad (34)$$

Notice that, as far as the calculation of the  $\langle \dots \rangle_0$  averages are concerned, all spins can be considered as statistically independent. Thus, the mean value of an arbitrary function of a spin placed in (say) the odd sublattice is simply

$$\langle f(\vec{\phi}) \rangle_0^{(\text{odd})} = \frac{\int_0^{2\pi} d\varphi \int_{-1}^1 d\phi^z f(\vec{\phi}) e^{-V_o(\phi^z)/T}}{\int_0^{2\pi} d\varphi \int_{-1}^1 d\phi^z e^{-V_o(\phi^z)/T}}, \quad (35)$$

$$\vec{\phi} = (\sqrt{1 - (\phi^z)^2} \cos \varphi, \sqrt{1 - (\phi^z)^2} \sin \varphi, \phi^z). \quad (36)$$

We now need to parametrize the local potentials with the help of the mean fields, that will be our minimizing parameters. One easily sees that keeping only the linear term ( $V_{e,o}(\phi^z) = h_{e,o}\phi^z$ ) will not reproduce the ferrimagnetic or antiferrimagnetic phases, since at very low temperatures and non vanishing mean-fields,  $h_{e,o}$ , the spins would always be (anti)aligned with the Z axis. If one keeps also the quadratic term,  $V_{e,o}(\phi^z) = h_{e,o}\phi^z + \lambda_{e,o}(\phi^z)^2$ , the situation improves significantly. The minimum of  $V_{e,o}$  can now be  $-1 \leq \phi_{\min}^z \leq 1$  which implies that at low temperature spins would lie on the cone of angle  $\theta$ ,  $\cos \theta = \phi_{\min}^z$ . Therefore, we will choose as our variational family

$$\begin{aligned} H_0 = & - \sum_{i \text{ even}} (h_e \phi_i^z + \lambda_e (\phi_i^z)^2) \\ & - \sum_{i \text{ odd}} (h_o \phi_i^z + \lambda_o (\phi_i^z)^2). \end{aligned} \quad (37)$$

As an extra-bonus, we find that the RP<sup>2</sup>-phase can be represented by this ansatz if the Mean Fields that minimize the r.h.s. of inequality (33) —at those particular  $T$  and  $J$  values— happen to be  $h_e = h_o = 0$ ,  $\lambda_e = -\lambda_o > 0$ . This can be explicitly checked by calculating the order parameters as a function of the mean-fields. Due to the symmetry between the even and odd sublattices, the expressions simplify in terms of the natural linear combinations of the Mean-Fields  $h_e, h_o, \lambda_e, \lambda_o$ :

$$\begin{aligned} h &= (h_e + h_o)/2, \\ h_s &= (h_e - h_o)/2, \\ \lambda &= (\lambda_e + \lambda_o)/2, \\ \lambda_s &= (\lambda_e - \lambda_o)/2. \end{aligned} \quad (38)$$

In terms of these variables, by means of a series expansion in  $h, h_s, \lambda$  and  $\lambda_s$ , one gets for the order parameters:

$$\begin{aligned} \mu^V &= \frac{1}{2}(\langle \phi^z \rangle_0^{(\text{even})} + \langle \phi^z \rangle_0^{(\text{odd})}) \\ &= \frac{2}{3}\beta h + \frac{8}{45}(h\lambda + h_s\lambda_s) + O(h^2, h_s^2, \lambda^2, \lambda_s^2), \end{aligned} \quad (39)$$

$$\begin{aligned} \mu_s^V &= \frac{1}{2}(\langle \phi^z \rangle_0^{(\text{even})} - \langle \phi^z \rangle_0^{(\text{odd})}) \\ &= \frac{2}{3}\beta h_s + \frac{8}{45}(h_s\lambda + h\lambda_s) + O(h^2, h_s^2, \lambda^2, \lambda_s^2), \end{aligned} \quad (40)$$

$$\begin{aligned} \mu^T &= \frac{1}{2} \left( \langle (\phi^z)^2 \rangle_0^{(\text{even})} + \langle (\phi^z)^2 \rangle_0^{(\text{odd})} \right) - \frac{1}{3} \\ &= \frac{4}{45}\beta\lambda + \frac{2}{45}\beta^2(h^2 + h_s^2) + \frac{4}{945}\beta^2(\lambda^2 + \lambda_s^2) \\ &\quad + O(h^2, h_s^2, \lambda^2, \lambda_s^2), \end{aligned} \quad (41)$$

$$\begin{aligned} \mu_s^T &= \frac{1}{2} \left( \langle (\phi^z)^2 \rangle_0^{(\text{even})} - \langle (\phi^z)^2 \rangle_0^{(\text{odd})} \right) \\ &= \frac{4}{45}\beta\lambda_s + \frac{1}{45}\beta^2 h h_s + \frac{8}{945}\beta^2 \lambda \lambda_s \\ &\quad + O(h^2, h_s^2, \lambda^2, \lambda_s^2). \end{aligned} \quad (42)$$

With this information in hand one can identify the different phases that we found at  $T = 0$  in terms of the non-vanishing Mean-Fields (of course the high-temperature PM phase corresponds to the vanishing of all four mean-fields!):

$$\begin{aligned} \text{FM : } & h > 0, h_s = \lambda = \lambda_s = 0, \\ \text{AFM : } & h_s > 0, h = \lambda = \lambda_s = 0, \\ \text{FI : } & h, \lambda_s > 0, h_s = \lambda = 0, \\ \text{AFI : } & h_s, \lambda > 0, h = \lambda_s = 0, \\ \text{RP}^2 : & \lambda_s > 0, h = h_s = \lambda = 0. \end{aligned} \quad (43)$$

Let us now describe the actual calculation. As previously said, we introduce the function

$$\Phi(h, h_s, \lambda, \lambda_s) = F_0 + \langle H - H_0 \rangle_0, \quad (44)$$

that, at its minimum as a function of  $h, h_s, \lambda$  and  $\lambda_s$ , we shall identify (in Mean-Field approximation) with the equilibrium free-energy. The partition function can be factorized to the contribution of the  $V/2$  points of the even sublattice and the  $V/2$  points of the odd sublattice:

$$Z_0 = Z_e^{V/2} Z_o^{V/2} = e^{-\beta F_0}, \quad (45)$$

where

$$Z_{e,o} = \int_0^{2\pi} d\varphi \int_{-1}^1 d\phi^z e^{\beta(h_{e,o}\phi^z + \lambda_{e,o}(\phi^z)^2)}, \quad (46)$$

$$F_0 = -\frac{V}{2\beta}(\log Z_e + \log Z_o). \quad (47)$$

The average of the Mean Field Hamiltonian is

$$\begin{aligned} \langle H_0 \rangle_0 &= -\frac{V}{2} \left[ h_e \langle \phi^z \rangle_0^{(\text{even})} + \lambda_e \langle (\phi^z)^2 \rangle_0^{(\text{even})} \right. \\ &\quad \left. + h_o \langle \phi^z \rangle_0^{(\text{odd})} + \lambda_o \langle (\phi^z)^2 \rangle_0^{(\text{odd})} \right]. \end{aligned} \quad (48)$$

As for the average of the true Hamiltonian, one finds:

$$\begin{aligned} \langle H \rangle_0 &= -3VJ \langle \phi^z \rangle_0^{(\text{even})} \langle \phi^z \rangle_0^{(\text{odd})} \\ &\quad - 3VJ \left\langle \sqrt{1 + \vec{\phi}_e \cdot \vec{\phi}_o} \right\rangle_0. \end{aligned} \quad (49)$$

In the above expression,  $\vec{\phi}_{e,o}$  is a generic spin belonging to the even (odd) sublattice. The problem is that, even if

$\vec{\phi}_e$  and  $\vec{\phi}_o$  are statistically independent, the calculation of the mean-value of the square root in Eq. (50) cannot be straightforwardly factorized in an even and an odd contribution. In order to achieve this factorization, we shall use the series expansions introduced by de Gennes.<sup>31</sup> One first use an expansion in Legendre Polynomials:

$$\sqrt{1 + \vec{\phi}_e \cdot \vec{\phi}_o} = \sum_{l=0}^{\infty} A_l P_l(\vec{\phi}_e \cdot \vec{\phi}_o), \quad (50)$$

$$A_l = (-1)^{l+1} \frac{2\sqrt{2}}{(2l-1)(2l+3)}. \quad (51)$$

We can now factorize the Legendre Polynomials using their expression in terms of spherical harmonics

$$P_l(\vec{\phi}_e \cdot \vec{\phi}_o) = \frac{4\pi}{2l+1} \sum_{m=-l}^l Y_l^{m*}(\phi_e^z, \varphi_e) Y_l^m(\phi_o^z, \varphi_o). \quad (52)$$

Thus, the mean-values are factorized into even and odd contributions. Due to the rotational symmetry along the Z axis, only the  $m = 0$  terms in Eq. (52) are non vanishing. Thus we obtain,

$$\langle P_l(\vec{\phi}_e \cdot \vec{\phi}_o) \rangle_0 = \langle P_l(\phi^z) \rangle_0^{(\text{even})} \langle P_l(\phi^z) \rangle_0^{(\text{odd})}. \quad (53)$$

Fortunately, if one wants to calculate the free-energy  $\Phi$  as a series expansion in the Mean-Fields,  $h$ ,  $h_s$ ,  $\lambda$  and  $\lambda_s$ , at a given order only a finite number of terms in Eq. (50) contribute, due to the orthogonality properties of the Legendre Polynomials. This expansion allows to discuss the continuous phase transitions from the PM phase (where  $h = h_s = \lambda = \lambda_s = 0$  is the absolute minimum of the free-energy), to ordered phases. Indeed, calculating  $\Phi$  (per unit volume) to second order one gets:

$$\begin{aligned} \frac{1}{V} \Phi(h, h_s, \lambda, \lambda_s) \approx & \left( \frac{\beta}{6} - \frac{J\beta^2}{3} - \frac{2\sqrt{2}\beta^2}{15} \right) h^2 \quad (54) \\ & + \left( \frac{\beta}{6} + \frac{J\beta^2}{3} + \frac{2\sqrt{2}\beta^2}{15} \right) h_s^2 \\ & + \left( \frac{8\sqrt{2}\beta^2}{1575} + \frac{2\beta}{45} \right) \lambda^2 \\ & + \left( -\frac{8\sqrt{2}\beta^2}{1575} + \frac{2\beta}{45} \right) \lambda_s^2. \end{aligned}$$

This is a quadratic form in  $h$ ,  $h_s$ ,  $\lambda$  and  $\lambda_s$ . If the above quadratic form is positive definite, the PM phase is a (local) minimum of the free energy. The other way around, when one of the eigenvalues of the quadratic form is negative, the PM phase is unstable with respect to some ordered phase, depending on the Mean-Field that should grow in order to minimize the free-energy. Notice also that the eigenvalue corresponding to  $\lambda^2$  is always positive. Thus, even if there are four eigenvalues, we obtain three lines of continuous phase transitions, where the eigenvalues vanish:

$$\begin{aligned} \text{PM-FM line: } & T = 2J + 4\sqrt{2}/5, \\ \text{PM-AFM line: } & T = -2J - 4\sqrt{2}/5, \\ \text{PM-RP2 line: } & T = 4\sqrt{2}/35. \end{aligned} \quad (55)$$

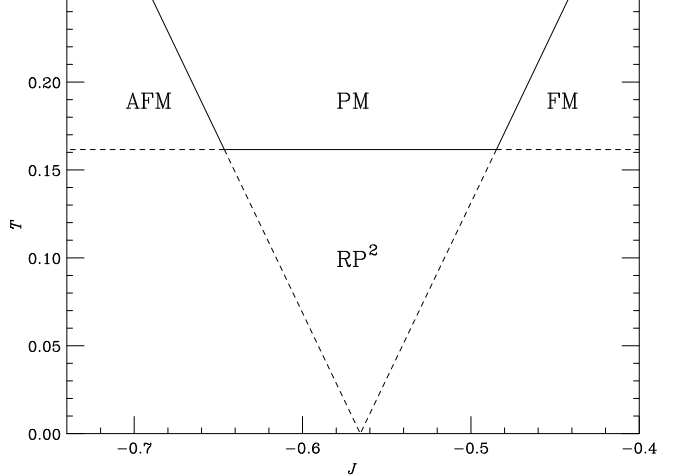


FIG. 1: Phase diagram as obtained from the second order series expansion of the free-energy (55). The paramagnetic phase is unstable for temperatures below the full-lines (the instability being toward the FM, AFM or RP<sup>2</sup> phases, as indicated in the plot). The dashed lines indicate the places where some of the eigenvalues of the quadratic form in (55) vanish, but they do not correspond to phase transitions.

Therefore the PM phase, stable at high-temperature, meets two transition lines of opposite slope, and an horizontal line that separates it from the RP<sup>2</sup> phase (see Fig. 1).

For temperatures below the full lines in Fig. 1, one needs to discuss the stability of a minimum of the free-energy different from  $h = h_s = \lambda = \lambda_s = 0$ . To locate that minimum, and to discuss its stability, one needs to extend the series expansion in (55) at least to fourth-order in  $h$ ,  $h_s$ ,  $\lambda$  and  $\lambda_s$ . This can be done (see Appendix B), but it is not particularly illuminating since the series expansion for  $\Phi$  is not fastly convergent. We have rather turned to a numerical method. Given a particular value of the Mean-Fields,  $h$ ,  $h_s$ ,  $\lambda$ ,  $\lambda_s$ , we have calculated  $\Phi$  by means of a Gauss-Legendre integration of all the terms in Eq. (44). To do this, we have divided the interval  $[-1, 1]$  in twelve subintervals and we have done a twelfth order Gauss-Legendre integration in each of them. The series of Eq. (50) has been evaluated to order 50. Being able to calculate  $\Phi$ , the minimization has been done using a conjugate gradient method. The resulting phase diagram is shown together with the results of the Monte Carlo calculation in Fig. 2. Notice that, as usual, the Mean-Field calculation overestimates the critical temperatures by a large factor (about 2.3 in this case). However, considering this rescaling of the temperatures, the obtained phase-diagram is in remarkable agreement with the numerical one. We have confirmed that all the transitions are second order except the ferromagnetic-RP2 which is first order (nevertheless, this transition line is an artifact of the Mean-Field solution: in the Monte Carlo phase-diagram it seems to collapse to a tetracritical point). The second order nature of the transitions

can be checked by computing the appropriate order parameter at a given value of  $T$  and  $J$ , then noticing that it vanishes at the transition line with Mean-Field exponents ( $M \propto |T - T_c|^{1/2}$  or  $\propto |J - J_c|^{1/2}$ ).

Since Mean-Field overestimates critical temperatures, it is interesting to compare the previous results with the ones of another approximation (large  $N$ ) that usually underestimates them. We have calculated the position of the PM-FM and PM-AFM phase-transition in the large  $N$  approximations (see Appendix A):

$$\begin{aligned} \text{PM-FM line: } T &= +1.2578 J + 0.5578, \\ \text{PM-AFM line: } T &= -1.2578 J - 0.793. \end{aligned} \quad (56)$$

The critical temperature is underestimated by roughly the same factor that the Mean Field approximation overestimates it (see below). To extend further this calculations would require to study non translationally invariant saddle-points, which is rather complex.

#### IV. MONTE CARLO SIMULATION

The model (1) can be investigated using a standard Monte Carlo method. We shall here describe some technical points, the results being discussed in the following subsections.

The single Monte Carlo (MC) step consists of a full-lattice Metropolis lattice sweep. Some of the simulations have been done at extremely low temperatures, thus the method of choice would have been a heat-bath algorithm, but its implementation in this model is rather complex. Fortunately, one can effectively falsify a heat-bath algorithm by means of a multi-hit Metropolis method, proposing per each hit as spin update a random spin on the unit sphere. Luckily enough, to achieve a 50% acceptance the number of needed hits is quite modest except for the lowest temperatures that represent a negligible fraction of the total CPU time devoted to the problem. The pseudo-random number generator was the Congruential+Parisi-Rapuano (see e.g. Ref. 32).

To extract critical exponents and critical temperatures, we have used the quotient methods:<sup>18,33</sup> for a pair of lattices of sizes  $L$  and  $2L$  we choose the temperature where the correlation-lengths in units of the lattice-size coincide ( $2\xi_L = \xi_{2L}$ ). Up to scaling corrections, the matching temperature is the critical point. Let now  $O$  be a generic observable diverging at the critical point like  $|t|^{-x_O}$ . Then, one has (up to scaling corrections<sup>18,33</sup>):

$$\left. \frac{\langle O \rangle_{2L}}{\langle O \rangle_L} \right|_{\frac{\xi_{2L}}{\xi_L} = 2} = 2^{x_O/\nu}, \quad (57)$$

where  $\nu$  is the critical exponent for the correlation length itself. For extracting  $\nu$  we have used the temperature derivative of the correlation-length,  $x_{\partial_T \xi} = 1 + \nu$ . To fulfill the matching condition  $2\xi_L = \xi_{2L}$  one often needs to extrapolate from the simulation temperature to a nearby one. This has been done using a reweighting method (see e.g. Ref. 34).

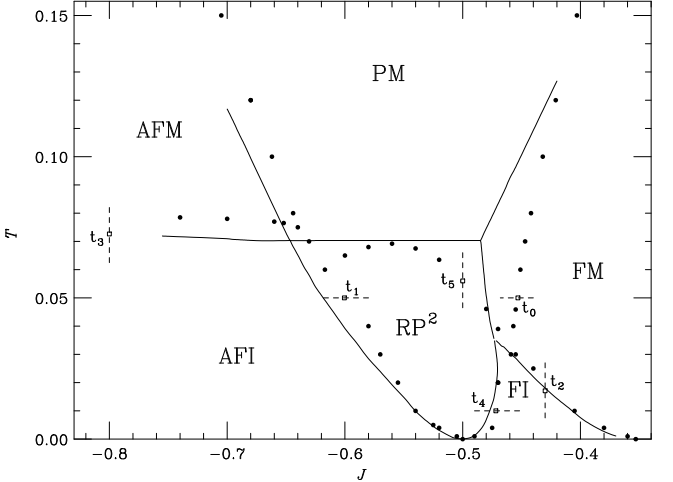


FIG. 2: Phase diagram of the model. Circles correspond to Monte Carlo estimates. Full lines correspond to the Mean-Field transition temperatures divided by 2.3. The dashed vertical and horizontal lines show the direction of the Ferrenberg-Swendsen extrapolation in the points which are the subject of detailed study reported. We label  $t_0 \dots t_5$  each one of the more carefully studied transitions.

#### A. Phase Diagram

At a first stage, the phase diagram (see Fig. 2) has been explored by performing hysteresis cycles with  $L$  from 6 to 24. The energy and relevant order parameters have been used to locate phase transitions. Once a rough diagram has been established, we have simulated in lattices  $L = 6, 12$ , and have refined the transition point calculating the correlation lengths associated to the relevant order parameter and computing the point where  $\xi/L$  is  $L$  independent. The phase diagram obtained can be seen in Fig. 2. We have studied in greater detail the phase transitions at the points  $t_0, \dots, t_5$ , depicted in Fig. 2. We have simulated lattices  $L = 6, 8, 12, 16, 24, 32, 48$  and 64, producing 20 million of MC full-lattice sweeps for the largest lattices in each transition. We have discarded  $5 \times 10^5$  MC steps for thermalization. In all cases this has been checked to be much larger than the integrated autocorrelation time. In addition, at the lowest temperatures, we have compared different starting configurations (random, FM, etc.), concluding that the results are start-independent.

Before discussing the results let us briefly comment what can one expect on universality grounds. Transition  $t_0$  connects the paramagnetic phase, where the full  $O(3)$  symmetry-group is preserved, to a FM phase where the symmetry group is just the  $O(2)$  group corresponding to the global rotations around the global magnetization. Thus it is expected (and confirmed) to be in the Universality class of the  $O(3)$  Non Linear  $\sigma$  model (see table III). For all the other transitions the scheme of symmetry breaking is not so clear. The only obvious symmetry-breaking (for transitions  $t_2$  and  $t_3$ ) is the

Transition	$L = 6$	$L = 8$	$L = 12$	$L = 16$	$L = 24$	$L = 32$
$t_0 (T = 0.05, \mu^V)$	-0.453561(15)	-0.453293(32)	-0.453131(19)	-0.453090(15)	-0.453091(29)	—
$t_1 (T = 0.05, \mu^V)$	-0.59828(8)	-0.59939(4)	-0.60015(2)	-0.60038(1)	-0.60043(2)	-0.60044(2)
$t_1 (T = 0.05, \mu_s^V)$	-0.60083(4)	-0.60084(3)	-0.60078(2)	-0.60067(1)	-0.60052(2)	-0.60048(2)
$t_2 (J = -0.43, \mu_s^V)$	0.017663(12)	0.017343(5)	0.017163(4)	0.017129(2)	0.017112(2)	0.017101(4)
$t_3 (J = -0.8, \mu^V)$	0.07528(4)	0.07387(2)	0.07304(2)	0.07283(1)	0.07267(1)	0.07260(1)
$t_4 (T = 0.01, \mu^V)$	-0.47199(3)	-0.47198(2)	-0.47196(2)	-0.47195(1)	-0.471919(6)	-0.471916(3)
$t_4 (T = 0.01, \mu_s^V)$	-0.47241(3)	-0.47219(3)	-0.47201(2)	-0.47196(1)	-0.471914(6)	-0.471912(3)

TABLE I:  $J_c$  or  $T_c$  determined by the intersection of the correlation lengths measured in two lattices of size  $L$  and  $2L$ .  $t_N(X, A)$  stands for:  $t_N$ , transition,  $X$  fixed parameter and  $A$  the order parameter associated with the correlation length considered.

Transition	$L = 6$	$L = 8$	$L = 12$	$L = 16$	$L = 24$	$L = 32$
$t_0 (T = 0.05, \mu^V)$	0.707(4)	0.702(7)	0.712(12)	0.710(10)	0.629(95)	—
$t_1 (T = 0.05, \mu^V)$	0.594(20)	0.556(7)	0.555(8)	0.540(8)	0.546(17)	0.596(25)
$t_1 (T = 0.05, \mu_s^V)$	0.592(5)	0.561(6)	0.538(5)	0.519(7)	0.517(13)	0.561(22)
$t_2 (J = -0.43, \mu_s^V)$	0.591(8)	0.569(5)	0.537(3)	0.548(5)	0.588(8)	0.604(17)
$t_3 (J = -0.8, \mu^V)$	0.583(10)	0.557(4)	0.562(3)	0.582(6)	0.605(7)	0.651(20)
$t_4 (T = 0.01, \mu^V)$	0.534(4)	0.536(10)	0.560(10)	0.597(15)	0.630(17)	0.656(24)
$t_4 (T = 0.01, \mu_s^V)$	0.545(7)	0.564(13)	0.581(13)	0.611(16)	0.629(17)	0.650(25)

TABLE II: Apparent  $\nu$  exponent obtained from the quotient method applied to  $(L, 2L)$  pairs.

symmetry between the even and odd sublattice. This is a  $Z_2$  symmetry, thus one might expect the transition to be in the Ising Universality class. The symmetries of the  $RP^2$  phase are intriguing and will be investigated in the following subsection. Let us only recall that the transition  $t_5$  has been recently studied in great detail in Ref. 4, where it was found that

$$T_c = 0.055895(5), \quad (58)$$

$$\nu = 0.781(18). \quad (59)$$

Perhaps not unexpectedly, the critical exponents were found to be compatible within errors with the one of the antiferromagnetic  $RP^2$  model.<sup>18</sup>

Model	$\nu$
$O(1)$ (Ising) <sup>35</sup>	0.6294(10)
$O(2)$ <sup>36</sup>	0.67155(27)
$O(3)$ <sup>37</sup>	0.710(2)
$O(4)$ <sup>37</sup>	0.749(2)
$RP^2$ -AFM <sup>18</sup>	0.783(11)
Chiral(Heisenberg) <sup>28</sup>	0.57(3)
Chiral(XY) <sup>28</sup>	0.55(3)
Tricritical <sup>5</sup>	1/2
Weak 1 <sup>st</sup> order <sup>38</sup>	1/2
1 <sup>st</sup> order	1/3

TABLE III: Critical exponent  $\nu$  for some three dimensional Universality Classes.

As for transitions  $t_0, \dots, t_4$ , we have located quite accurately the critical parameters (see table I). We have focused in each case in the largest order parameter (see

Eq. (22)). The PM-AFM transition should have the same critical behavior and we have not invested time in this study. We are reasonably confident in the continuous nature of all five transitions. This stems from two facts. First, the energy histograms are not double-peaked (see an example in Fig. 3). Yet, a much more refined test comes from the ( $L$ -dependent) value of the effective  $\nu$  exponents shown in table II. With the exception of transition  $t_0$ , which as expected belongs to the Universality Class of the Heisenberg model in three dimensions, scaling-corrections are not even monotonous in their evolution with the lattice size. Although an asymptotic value can not be guessed with reachable lattice sizes, at least one sees that, for the largest lattices, the exponent  $\nu$  is reasonably far from the value 1/2 to be expected in weak first order transitions.

## B. Detailed study of the $RP^2$ phase

The  $RP^2$  phase poses many questions, the first one possibly being: is it truly a  $RP^2$  phase? In other words, (as far as long-distance correlations are concerned) do the spins behave like *segments* rather than *arrows*? As we will see below, the answer is positive: the spin ordering is truly invariant under spin reversal. Once this is established, one may worry about continuous symmetries. At the special point  $T = 0$ ,  $J = -0.5$ , the spins in the (say) even sublattice are randomly aligned or anti-aligned with the (say) Z-axis. The spins in the odd sublattice are randomly placed on the XY-plane. This state has a remaining  $O(2)$  symmetry, corresponding to rotations around the Z-axis. The  $Z_2$  symmetry corresponding to

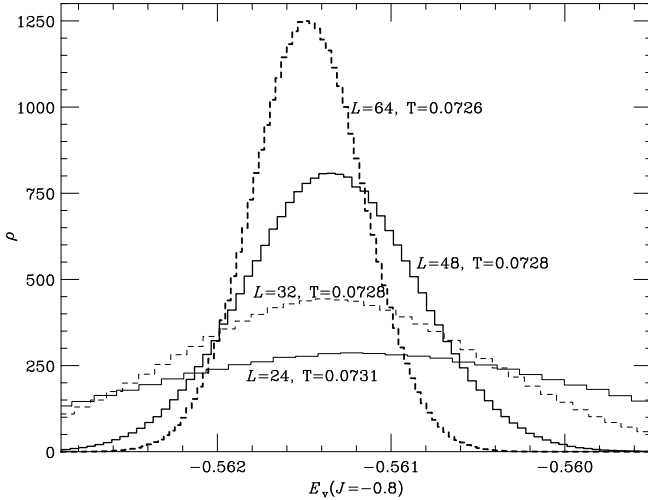


FIG. 3: Histogram for  $E_v = \langle \vec{\phi}_i \cdot \vec{\phi}_j \rangle$  (for nearest neighbors  $i$  and  $j$ ), in transition  $t_3$ .

exchanging the roles of the even and odd sublattices is obviously broken. Hence one may wonder if, up to the critical temperature which separates it from the paramagnetic state, the RP<sup>2</sup> phase can be characterized as an O(2)-symmetric phase with broken even-odd symmetry. Doubts arise from the order-from-disorder interaction that favors the alignment<sup>18</sup> (in the segment sense) of all the spins in the planar sublattice (the odd sublattice in the above discussion). This global alignment would imply a second phase transition separating the low temperature O(2)-symmetric phase from a phase without any remaining rotational symmetry at higher temperature. This second RP<sup>2</sup> phase would be separated from the paramagnetic state where the full rotational symmetry, O(3), is maintained. This complex scenario would explain the exotic values of the critical exponents corresponding to the RP<sup>2</sup>-PM transitions. Universality arguments<sup>25</sup> would then predict that the critical exponents would be the ones of the O(4) classical Non-Linear  $\sigma$  model, which are not very far from the ones actually found<sup>4</sup>. On the other hand, in the simple scenario of a single O(2) symmetric RP<sup>2</sup> phase, the expected critical exponents would be those of the classical Heisenberg model, in plain contradiction with our numerical results. Since the simple scenario seems to be the real one, we are facing a failure of the Universality Hypothesis for which we do not have any plausible explanation.

To summarize, in the following we shall address, in this order, the three following questions:

1. Is the RP<sup>2</sup> phase truly segment-like?
2. Is the even-odd symmetry broken up to the temperature separating the RP<sup>2</sup> phase from the Paramagnetic state?
3. Is the low temperature O(2) symmetric RP<sup>2</sup> phase preserved up to the temperature separating the

RP<sup>2</sup> phase from the Paramagnetic state?

### 1. Tensor versus vector ordering

We have called RP<sup>2</sup> the phase in which the vector magnetization vanishes (for any momentum in the Brillouin zone), and the tensor magnetization is non-vanishing, both at momentum  $(0, 0, 0)$  ( $\mu^T$ ) and at momentum  $(\pi, \pi, \pi)$  ( $\mu_s^T$ ). In Fig. 4 (upper and middle part) we show, fixing  $J = -0.5$ , that, for temperatures ranging from 0.001 to 0.05, there is a non vanishing thermodynamic limit for both quantities. For comparison, we show in the lower part the vector magnetization at momentum  $(\pi, \pi, \pi)$  ( $\mu_s^V$ ), which goes to zero as  $1/\sqrt{L^3}$ . We have also measured the correlation-length in the vector channel. Although some short-range ordering is present, the correlation-length is not larger than 0.3 lattice spacing.

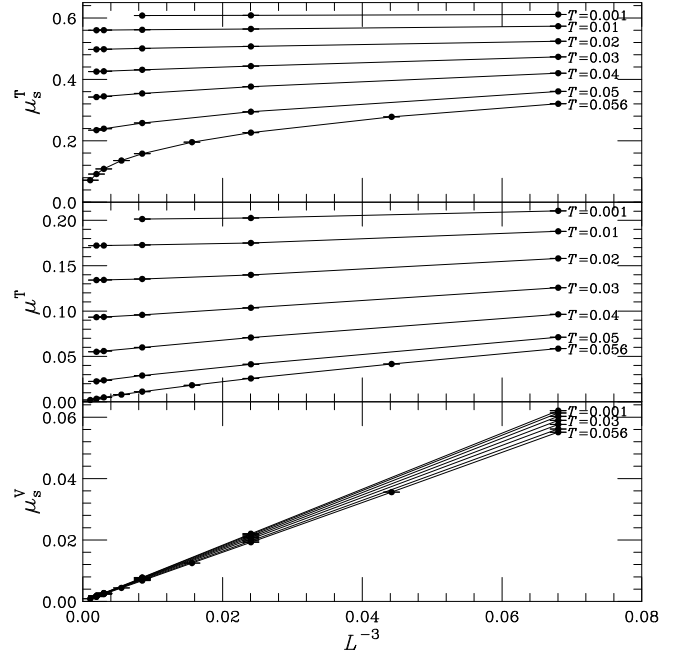


FIG. 4: Lattice size dependence of  $\mu_s^T$ ,  $\mu^T$  and  $\mu_s^V$  at different temperatures, for  $J = -0.5$ .

To confirm the absence of any other vectorial magnetization we have measured at  $J = -0.55, T = 0.5$  (just in the middle of the RP<sup>2</sup> phase) all Fourier components of the vector field  $\vec{\phi}_i$  for 90 statistically independent configurations for each lattice size, and plotted in Fig. 5 the corresponding momentum versus the maximum value of the Fourier component squared. In other words, we are searching for the maximum (over the Brillouin zone) of the static structure factor (divided by  $L^3$ ). We have chosen as lattice sizes  $L = 6, 8, 12, 30, 60$  to allow for different periodicities of the would-be vector-ordered states. If no vectorial ordering is present, the last quantity should go to zero as  $1/L^3$ , up to logarithmic corrections that arise from the fact that we are computing the maximum of a

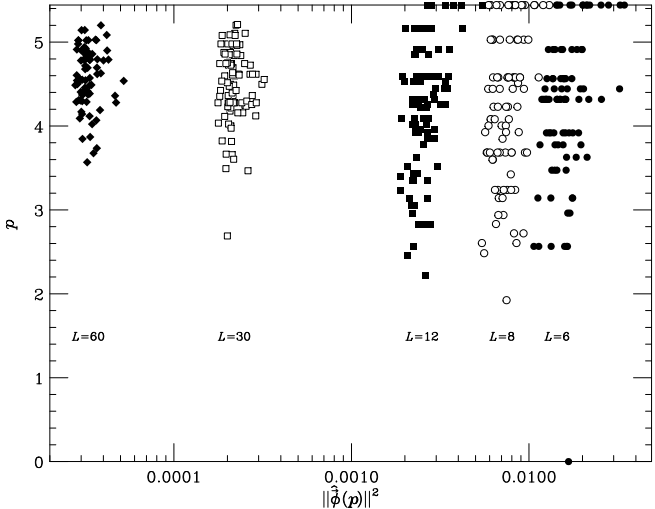


FIG. 5: Scatter-plot for 90 statistically independent configurations for each lattice size ( $L = 6, 8, 12, 30, 60$ ) at  $J = -0.55$ ,  $T = 0.5$ . In the horizontal axis we plot the maximum over the Brillouin zone of the squared Fourier transform of the spin field, and in the vertical axis the corresponding associated momentum  $p = \|\mathbf{p}\|$ . The horizontal position of legends scales as  $L^{-3} \log L$  in agreement with the absence-of-order prediction.

set of  $O(L^3)$  elements. The absence of ordering is clear from Fig. 5.

## 2. Even-Odd symmetry

To analyze the even-odd symmetry, we measure the tensor correlation difference at second neighbors between even and odd lattices. The normalized total difference for a given configuration can be written as

$$\Delta_E = \frac{2}{3L^3} \left( \sum_{\text{even}} (\phi_i \cdot \phi_j)^2 - \sum_{\text{odd}} (\phi_i \cdot \phi_j)^2 \right), \quad (60)$$

where the sums extend over even (odd) second neighbor pairs. The non-vanishing of the difference in the thermodynamic limit signals even-odd symmetry breaking. Notice that the sublattice energy difference can be defined locally, and it plays the role of a local field. Another interesting observable is the dimensionless quantity associated to the energy difference

$$\kappa_E = \frac{\langle \Delta_E^2 \rangle}{\langle \Delta_E \rangle^2}. \quad (61)$$

Fig. 6 shows the tensor energy difference as a function of temperature for several lattice sizes. A clear thermodynamic limit can be observed for  $T < 0.05$ . At  $T = 0.05$  the asymptotic behavior can be elucidated by a direct study of the tensor energy difference histograms. A  $L = 96$  lattice is necessary to clearly resolve the two peak structure of the histogram (see Fig. 7), corresponding to

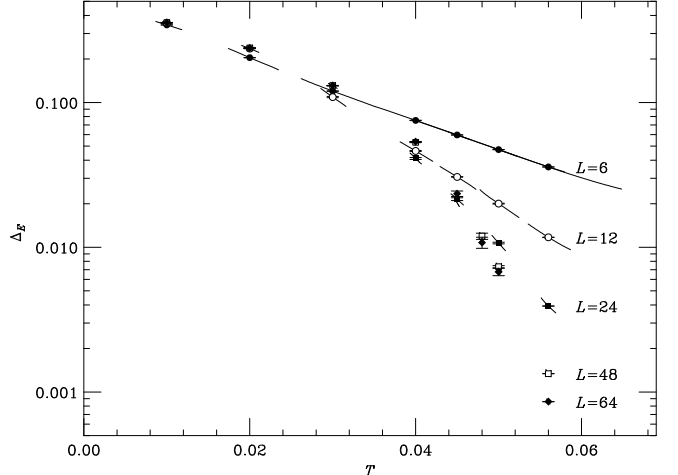


FIG. 6: Difference of the tensor second neighbors energies between sublattices, for  $T = 0.05$ .

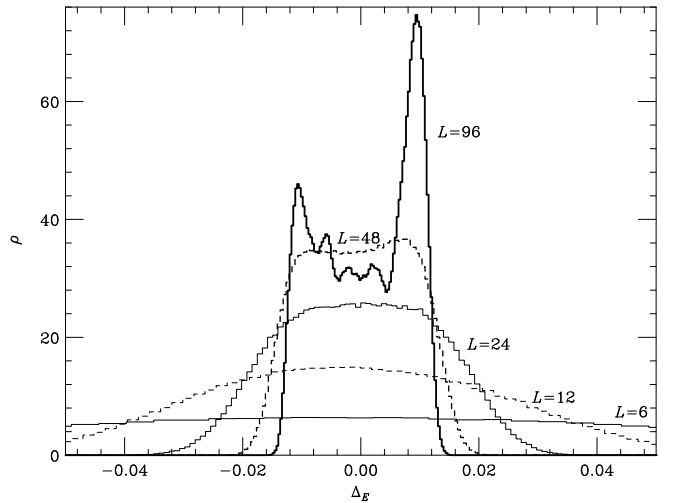


FIG. 7: Histogram of  $\Delta_E$  for  $J = 0.5$ ,  $T = 0.05$ .

an even-odd symmetry breaking. Notice that  $L = 96$  is the largest lattice used, which makes it impossible to study the thermodynamic limit of that quantity for  $T$  larger than 0.05 and less than  $T_c = 0.0559$ . We can conclude that, within the computational resources employed, no evidence exists for a thermodynamic limit with unbroken even-odd symmetry.

Although no thermodynamic limit can be reached beyond  $T = 0.05$ , more information can be obtained through a finite size analysis. The closer we get to  $T = 0.05$ , the harder it becomes to find a two peak structure in the histogram. A correlation length could be defined in the even-odd symmetry breaking channel which grows as the possible critical point between the  $\text{RP}^2$  phase with broken even-odd symmetry and a hypothetical  $\text{RP}^2$  phase with restored even-odd symmetry is approached. The functional form of the growth of the correlation length might give indication of the existence

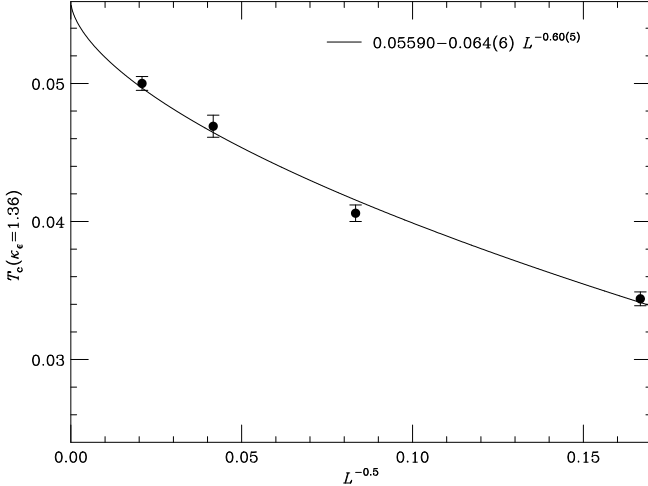


FIG. 8: Displacement of the critical temperature, defined as the point where  $\kappa_E$  takes a fixed value, as a function of size. Fits suggest that there is no even-odd symmetry restoration at a temperature less than the RP<sup>2</sup>-PM one.

of such phase transition. A direct way to carry out that study is to define the correlation length as the lattice-size itself, when the histogram has a central valley at half the peak height. The result shows a growth of the correlation length as  $T$  increases compatible with a divergence just at  $T_c$ , though with rather peculiar exponents. But the measurement of that correlation length is very noisy. A much more precise way to study the possible presence of a transition previous to  $T_c$  is to define as apparent critical point the  $T$  value at which  $\kappa_E$  takes a fixed value. Fig. 8 shows the results. Although the possibility of an even-odd symmetry recovery transition previous to  $T_c$  cannot be discarded, results are compatible with a divergence just at  $T_c$ . The figures show a fit to a power law (fixing the critical point to the value given in Eq. (58)). It is worth remarking that the  $\nu$  exponent obtained is very large (2 or larger), which might point to a logarithmic divergence. Thus, all our results point to a single RP<sup>2</sup> phase with broken even-odd symmetries at all temperatures.

### 3. $O(2)$ Symmetry

The chosen tool to study whether the  $O(2)$  symmetry of the  $T = 0$  state is preserved at higher temperatures, has been the eigenvalue structure of the tensor  $M_s$ . The latter being traceless implies that the vector  $\lambda = (\lambda_1, \lambda_2, \lambda_3)$  must lie on the  $x + y + z = 0$  plane. The whole information reduces, then, to a modulus (which is nothing but the observable  $\mu_s$ ), and an angle, which contains all the information of the eigenvalues on the symmetry  $O(2)$ . As any result must be symmetric under eigenvalue permutations and global inversion, we can restrict the angle to the interval between 0 and  $\pi/6$ . More

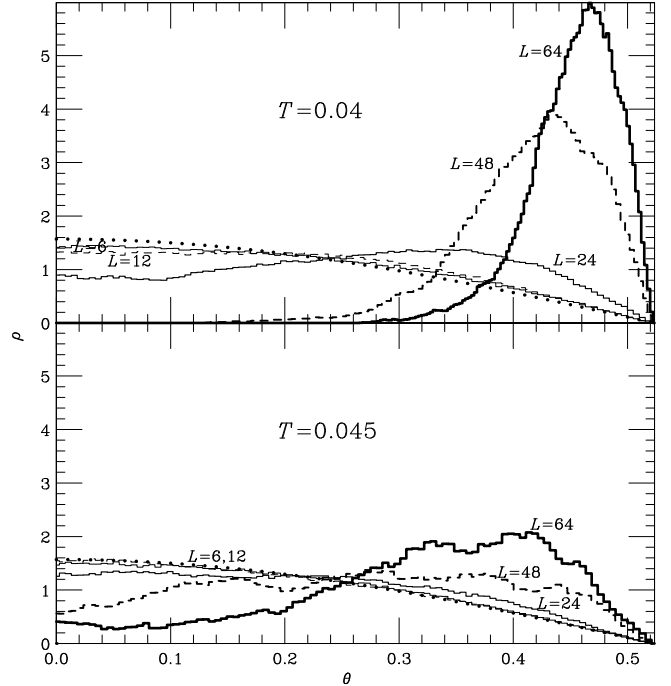


FIG. 9: Histograms of the angle of the eigenvalue vector on the (1,1,1) plane for two temperatures at  $J = -0.5$ . The dots correspond to paramagnetic configurations.

precisely, we consider the orthonormal basis  $\{\mathbf{u}_x, \mathbf{u}_y\}$  for the plane given by

$$\mathbf{u}_x = \frac{1}{\sqrt{2}}(-1, 1, 0) , \quad (62)$$

$$\mathbf{u}_y = \frac{1}{\sqrt{6}}(-1, -1, 2) . \quad (63)$$

and define the angle  $\theta$  from the relation

$$\tan \theta = \frac{\lambda \cdot \mathbf{u}_y}{\lambda \cdot \mathbf{u}_x} , \quad (64)$$

with the proviso that we choose a permutation and a global sign such that  $\theta$  lies between 0 and  $\pi/6$ .

Another interesting quantity can be defined as follows. In the thermodynamic limit an  $O(2)$ -symmetric phase corresponds to  $\lambda_2 = \lambda_3$ . We thus define

$$\Delta_\lambda = |\lambda_2 - \lambda_3| . \quad (65)$$

which must vanish in the thermodynamic limit if the  $O(2)$  symmetry is not broken. As usual the corresponding dimensionless quantity is

$$\kappa_\lambda = \frac{\langle \Delta_\lambda^2 \rangle}{\langle \Delta_\lambda \rangle^2} . \quad (66)$$

Fig. 9 shows histograms of angles at several temperatures and lattice sizes. Dotted lines correspond to completely disordered configurations. In case of the system being  $O(2)$ -symmetric (one large eigenvalue and two

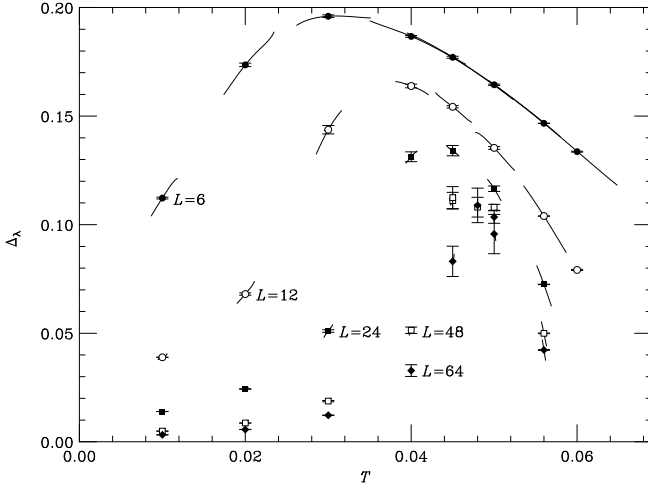


FIG. 10: Modulus of the difference between the two smaller eigenvalues of  $M_s$  as a function of  $T$ .

identical small eigenvalues), the distribution should be a delta at angle  $\pi/6$ . For a system with broken O(2)-symmetry but unbroken even-odd-symmetry, the eigenvalues are  $(a, 0, -a)$ -like, which would correspond to a Dirac delta at angle 0. We notice that, for small lattices, the distribution points to complete disorder, but as the size grows an inflection point turns up at  $T = 0.04, 0.045$  for  $L = 24, 48$  respectively, and as  $L$  goes on growing a peak arises at angles ever closer to the maximum. It might be said, that the behavior in  $L$  is always the same, except for a scale change.

Another interesting quantity is the difference between the two small eigenvalues ( $\Delta_\lambda$ ), which should vanish in the presence of O(2) symmetry, so turning out to be an order parameter. Fig. 10 shows that quantity for several values of the temperature and lattice size. If we look at an intermediate size ( $L = 24$  for instance) the appearance is that of a transition at  $T = 0.03$  to a phase with broken O(2) symmetry. Yet, as  $L$  increases, the apparent transition moves back approaching  $T_c$  ever more.

To check the consistency of the results with respect to the existence of a transition within the RP<sup>2</sup> phase we can perform a Finite Size Scaling study fitting  $\Delta_\lambda L^{\beta/\nu}$  as a function of  $(T - T_0)L^{1/\nu}$ . Only  $T_0 = T_c$  yields a reasonable fit (see Fig. 11). Notice that for  $T$  close to  $T_c$  the definition of  $\Delta_\lambda$  ceases to be meaningful, as a large eigenvalue exists no more since the RP<sup>2</sup> magnetization fades away, and no good fit can be expected. However, for most  $T$  values (more precisely, for  $T < 0.05$ ) the fit is excellent, though the  $\eta$  and  $\nu$  values are admittedly rather unusual ( $\eta = -0.5, \nu = 1.8$ ). The conclusion should be that there is no evidence for an O(2) breaking transition at any finite distance from  $T_c$ . A collapse of that transition over the RP<sup>2</sup>-PM transition might occur.

A more quantitative analysis can be made studying the displacement of the temperature at a fixed value of  $\kappa_\lambda$ . In Fig. 12 we plot the obtained measures together with fits

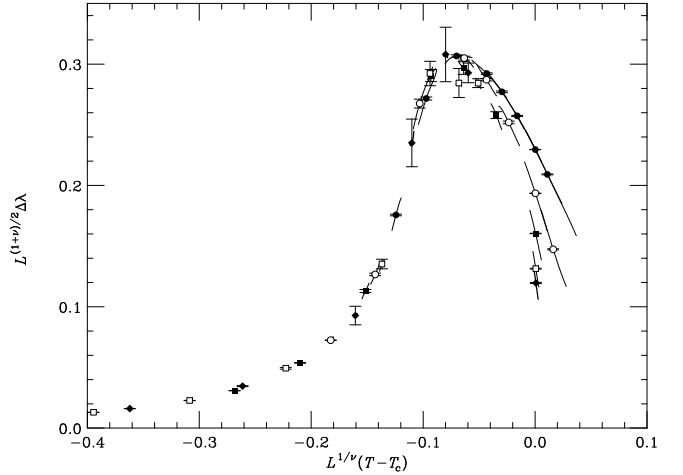


FIG. 11: Scaling of  $\Delta_\lambda$  for the analysis of a possible O(2) restoring transition. Data is fairly well fitted assuming the transition occurs at  $T_c$  (Points next to  $T_c$  are not well fitted because there the largest eigenvalue becomes zero and  $\Delta_\lambda$  ceases to make sense). The fitted values are  $\eta = -0.5, \nu = 1.8, T_c = 0.0559$ .

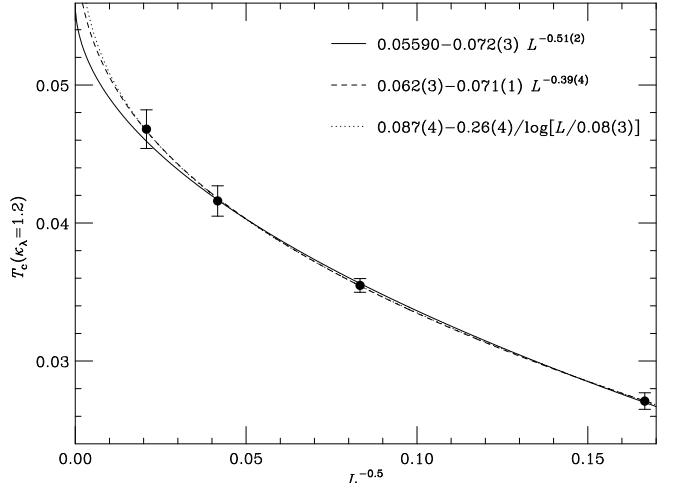


FIG. 12: Displacement of the critical temperature, defined as the point where  $\kappa_\lambda$  takes a fixed value, as a function of size. Fits suggest that there is no O(2) breaking transition, at a temperature less than the RP<sup>2</sup>-PM transition temperature.

to several functional forms: a power law with  $T_c$  fixed to the value of Eq. (58), a three parameter power law, and a Kosterlitz-Thouless-like divergence. The results point again to no breaking of the O(2) symmetry inside the RP<sup>2</sup> phase.

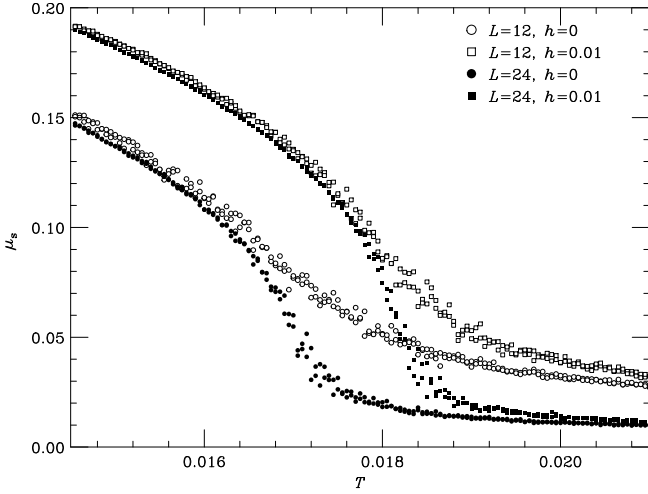


FIG. 13: Hysteresis along  $t_2$ . The transition occurs in the region where  $\mu_s^V$  changes suddenly, and the figure shows a movement of  $T_c$  to higher values when  $h = 0.01$  is switched on ( $T_c(h = 0) = 0.0171$ ).

### C. Interplay between Ferromagnetism, Antiferromagnetism, Temperature and an applied Magnetic Field in the low-doped $\text{La}_{1-x}\text{Sr}_x\text{MnO}_3$ .

In a series of papers<sup>21,22,23,24</sup> the interplay between FM, AFM, temperature and an applied magnetic field in the low-doped  $\text{La}_{1-x}\text{Sr}_x\text{MnO}_3$ , mainly at  $x$  close to  $1/8$ , has been studied. We would like to point out some properties of our FM-FI phase transition (point  $t_2$  in this paper) which might help to understand phenomena which, in those references, are related to the FM-CO (Charge Ordered) phase transition, not fully understood so far.

Roughly speaking, some of the mentioned phenomena are:

1. Resistance increases as  $T$  decreases below  $T_{\text{CO}}$  ( $t_2$  in our model). In our simplified model, this corresponds to the fact that, when crossing the FM-FI transition, odd and even spins cease to be aligned, which makes conductivity via DEM harder.
2. The Charge Ordered phase grows larger when an external magnetic field is applied. In our case, we have run a simulation with non zero magnetic field to see how the transition line moves.
3. In the CO phase, at fixed temperature, the magnetization increases with an external magnetic field, just as in a FM phase.

Let us now describe the physics of the FM-FI transition. Near the FM-FI transition, in the FM phase the ordering is symmetric with respect to the odd-even exchange and the field fluctuates at random around the total magnetization vector, the fluctuations being larger than in the FI phase, as shown by measurements of specific heats and susceptibilities made in both phases. More

precisely, the magnetization increases as the temperature goes down from the FM to the FI phase, which can be explained by a diminution of fluctuations. In fact, one would expect that the magnetization should be smaller in the FI phase, with fixed odds and evens on an open cone around the odd direction, than in the FM phase, where the evens lie on a narrower cone, with a larger projection on the odd direction. Yet, the large fluctuations in the FM phase destroy the even contribution to the magnetization. The FI vacuum consists then on the odd, practically frozen, sublattice, and the even sublattice, with spins on an open, but less fluctuating cone.

Let us now look in the FM phase close to the FI transition, and switch on a weak magnetic field in the Z direction. This will have the general effect of collimating the spins. In more detail, odd spins shall freeze closer to the Z direction, which shall cause the even sublattice to freeze on the cone, with smaller fluctuations. Paradoxically, the collimating effect of the magnetic field in the Z direction is to stabilize the cone, effectively opening it, giving rise to a more FI-like ordering, i.e., *the FI phase shall invade the FM phase, and the critical temperature shall rise*. This phenomenon (see point 2) is accompanied by an increase in the magnetization at fixed temperature in the FI phase (see point 3).

In order to check the correctness of the description, we have simulated in the neighborhood of the transition with  $h = 0.01$ , which does not alter the system properties, and have run a hysteresis cycle at  $J = -0.43$  in  $L = 12, 24$  between  $T = 0.01$  and  $T = 0.025$  (i.e. along  $t_2$ ). A good observable for the transition is  $\mu_s^V$ . The results at the two  $L$  values show that the finite size effects are negligible in front of the change in  $T_c$  with  $h$ .

Fig. 13 shows the result, which confirms that the inclusion of a magnetic field rises  $T_c$ , causing the invasion of the FI ordering into regions which at  $h = 0$  were FM.

## V. CONCLUSIONS

We have studied a simple model for double exchange interactions which retains a good number of interesting properties. It exhibits a complex phase diagram with ferromagnetic, ferrimagnetic phases, with their staggered counterparts, and a segment-ordered phase.

We obtain quantitatively all phases with approximate calculations (Mean Field and  $1/N$  expansions), which can be contrasted with *exact* Monte Carlo calculations. With Monte Carlo simulations we obtain, in addition to the precise positions of the transitions, information about their order. Our conclusion is that all transitions seem to be second order, although an accurate determination of the critical exponents is difficult and it is beyond the scope of this paper.

We have studied in detail the *exotic*  $\text{RP}^2$  phase (segment-ordered), concluding that it is a single phase up to the resolution allowed by the lattice sizes used in the simulation. The presence of a  $\text{RP}^2$  phase up to  $T = 0$

is interesting from the experimental point of view, since it can be confused with a PM or glassy phase and consequently with a Quantum Critical Point. We have shown that the structure factor ( $V$ , in fig. 5) remains bounded in the full Brillouin-zone. Therefore the RP<sup>2</sup> phase cannot be detected in neutron scattering experiments as a long-range ordering, although the phase transition will show up as a maximum (more precisely, a cusp) of the specific heat. A short-range ordering would of course always be present. Since the critical exponent  $\alpha$  is negative, the Harris criterion<sup>39</sup> implies that our results are robust against disorder effects. The RP<sup>2</sup> phase is characterized by a breakdown of the even-odd symmetry and a remaining O(2) symmetry, despite the fact that the measured critical exponents for the RP<sup>2</sup> transition point to a total breakdown of the initial O(3) symmetry. We have also discussed the effects of a magnetic field on the ferromagnetic-ferrimagnetic transition, and we have discussed its interplay with electrical conductivity.

### Acknowledgments

It is a pleasure to thank F. Guinea for useful conversation at the beginning of this work. We have maintained interesting discussions with A. Pelissetto regarding the large  $N$  approximation. This work has been partially supported through research contracts FPA2001-1813, FPA2000-0956, BFM2001-0718, BFM2003-8532, PB98-0842 (MCyT) and HPRN-CT-2002-00307 (EU). V. M.-M. is a Ramón y Cajal research fellow (MCyT) and S. J. is a DGA fellow. We have used the PentiumIV cluster RTN3 at the Universidad de Zaragoza for the simulations.

### APPENDIX A: LARGE $N$ APPROXIMATION

We write the model as

$$\mathcal{H} = -N \sum_{\langle i,j \rangle} W(1 + \vec{\phi}_i \cdot \vec{\phi}_j). \quad (\text{A1})$$

The Boltzmann weight is  $\exp(-\mathcal{H})$  and

$$W(x) = Jx + \sqrt{x}. \quad (\text{A2})$$

Using the expression of the Dirac deltas (one to fix the spin modulus,  $\vec{\phi}_i^2 = 1$ , and another to write that  $x = \vec{\phi}_i \cdot \vec{\phi}_j$ ) in terms of functional integrals, we can write the partition function of the model in the following way:<sup>40,41</sup>

$$\mathcal{Z} \propto \int d[\rho, \lambda, \mu, \vec{\phi}] e^{NA}, \quad (\text{A3})$$

with  $A$ , that action, as:

$$A = \frac{\beta}{2} \sum_{\langle i,j \rangle} \left( \lambda_{ij} + \lambda_{ij} \vec{\phi}_i \cdot \vec{\phi}_j - \lambda_{ij} \rho_{ij} + 2W(\rho_{ij}) \right) - \frac{\beta}{2} \sum_i \mu_i \left( \vec{\phi}_i^2 - 1 \right). \quad (\text{A4})$$

As we are interested (in this part of the calculation) in paramagnetic or/and ferromagnetic phases, we separate the spin in two pieces: the first one parallel to the symmetry breaking direction,  $\phi^{\parallel}$  (one degree of freedom), and the orthogonal part ( $N - 1$  degrees of freedom),  $\vec{\phi}^{\perp}$ . At this point, the spins have no definite modulus, and we can perform the functional integration over the orthogonal part of spins (a Gaussian integral)

$$\int d[\vec{\phi}^{\perp}] e^{-\frac{1}{2} \vec{\phi}^{\perp} \cdot \hat{R} \vec{\phi}^{\perp}} \propto \exp \left( -\frac{N-1}{2} \text{Tr} \log \hat{R} \right), \quad (\text{A5})$$

where  $R_{ij}^{ab}$  is the propagator ( $a, b = 1, \dots, N-1$  and  $i$  lives in the three-dimensional lattice) and it is given by

$$R_{ij}^{ab} = \delta^{ab} \beta \left( \beta \mu_i \delta_{ij} - \frac{1}{2} \sum_{\nu} \lambda_{ij} \delta_{i\nu j} \right). \quad (\text{A6})$$

The sum runs back and forth along the 3 lattice axes and  $i_{\nu}$  is the neighbor of site  $i$  in the direction defined by  $\nu$ . The trace,  $\text{Tr}$ , is over the space and spin components. The quantity  $\frac{1}{2}(\vec{\phi}^{\perp} \cdot \hat{R} \vec{\phi}^{\perp})$  is the contribution to  $A$  involving the orthogonal part of the spins (which is a quadratic form with matrix  $\hat{R}$ ).

In momentum space,  $\hat{R}$  reads:

$$R^{ab}(\mathbf{q}, \mathbf{q}') = \delta^{ab} \frac{\beta}{V} \sum_i e^{i(\mathbf{q}-\mathbf{q}') \cdot \mathbf{r}_i} \times \left( \mu_i - \frac{1}{2} \sum_{\nu} [\lambda_{ii\nu} e^{i\mathbf{q}' \cdot \nu} + \lambda_{i-\nu i} e^{-i\mathbf{q}' \cdot \nu}] \right), \quad (\text{A7})$$

where  $\nu = \mathbf{r}_{i\nu} - \mathbf{r}_{i-}$ . In the large  $N$  technique we must maximize  $A$ . In order to keep the computation at its simplest level, we make an ansatz over the fields  $\lambda_{ij}$ ,  $\mu_i$ ,  $\rho_{ij}$ , and  $\phi^{\parallel}$ : we are assuming that we will describe under this ansatz translational invariant phases, like paramagnetic and ferromagnetic ones. So, we will consider that all these fields are independent of  $x$  and  $\mu$  and we will write them as  $\lambda$ ,  $\rho$ ,  $\mu$  and  $\sigma$ . Therefore,  $A$  is

$$\frac{A}{V} = \frac{\beta}{2} d [\lambda(1 - \rho) + \lambda \sigma^2 + 2W(\rho)] + \frac{\beta}{2} \mu(1 - \sigma^2) - \frac{1}{2} \int dq \log \left[ \mu - \lambda \sum_{\nu} \cos q_{\nu} \right], \quad (\text{A8})$$

where  $d$  is the dimension of space and

$$\int dq \equiv \int_{[0, 2\pi)^d} \frac{d^d q}{(2\pi)^d} = 1. \quad (\text{A9})$$

Hence, this computation is valid in paramagnetic/ferromagnetic phases where we have translational invariance. As usual we write

$$\hat{p}^2 \equiv 4 \sum_{\nu} \sin^2(p_{\nu}/2). \quad (\text{A10})$$

The continuum limit of  $\hat{p}^2$  is  $p^2$ , and so, we can define a mass  $m_0$ :

$$m_0^2 = \frac{2\mu}{\lambda} - 2d. \quad (\text{A11})$$

and  $A$  can be written as

$$\begin{aligned} \frac{A}{V} = & \frac{\beta}{2}d[\lambda(1-\rho) + \lambda\sigma^2 + 2W(\rho)] + \frac{\beta}{2}\mu(1-\sigma^2) \\ & - \frac{1}{2}\log\lambda - \frac{1}{2}\int dq \log[m_0^2 + \hat{p}^2]. \end{aligned} \quad (\text{A12})$$

The saddle point equations are:

$$\beta d(1-\rho) + \frac{1}{\lambda}[(m_0^2 + 2d)I(m_0^2) - 1] + d\beta\sigma^2 = 0, \quad (\text{A13})$$

$$\beta(1-\sigma^2) = \frac{2}{\lambda}I(m_0^2), \quad (\text{A14})$$

$$2W'(\rho) = \lambda, \quad (\text{A15})$$

$$\sigma(d\lambda - \mu) = 0, \quad (\text{A16})$$

where

$$I(m_0^2) \equiv \int dq \frac{1}{m_0^2 + \hat{p}^2}. \quad (\text{A17})$$

One solution is  $\sigma = 0$ , the paramagnetic phase. We can find a second order phase transition by fixing the mass  $m_0$  to zero:

$$TI(0) = J + \frac{1}{2\sqrt{\rho_0}}, \quad (\text{A18})$$

where

$$\rho_0 = 2 - \frac{1}{2dI(0)}. \quad (\text{A19})$$

In three dimensions  $I(0) \simeq 0.2527$ . So we have found the critical line between the paramagnetic and ferromagnetic phases. This solution is only valid in  $J \geq -1/2$ . It is easy to check that the  $J = -1/2$  vertical line corresponds to infinite mass. So, with these formulas we cannot reach the region to the left of  $J = -1/2$ . Below we will see how to solve this drawback.

We can try to connect this calculation with the  $T = 0$  results. The solution  $\sigma \neq 0$  implies that  $d\lambda = \mu$  and so  $m_0^2 = 0$ . Notice that in a magnetized phase,  $m_0$  has no

longer the meaning of a mass (hence, in this case,  $m_0 = 0$  is not a signature of criticality). In this case the complete solution is:

$$\rho^* = 2 - \frac{1 - \sigma^2}{2I(0)d}, \quad (\text{A20})$$

and

$$T = \frac{1 - \sigma^2}{I(0)} \left[ J + \frac{1}{2\sqrt{\rho^*}} \right]. \quad (\text{A21})$$

This last equation tells us what is the magnetization  $1 - \sigma^2$  in a given point  $(T, J)$ . In the interval  $J > -1/2$  we obtain the solution  $\sigma = 1$ . In addition in the interval  $J \in (-1/2, -1/(2\sqrt{2}))$  a second solution with  $\sigma < 1$  appears. This is the signature of the ferrimagnetic phase. Hence, we have recovered part of the previous  $T = 0$  results.

As mentioned, above the previous calculation is valid only in paramagnetic/ferromagnetic phases. In order to manage the paramagnetic/antiferromagnetic phases we use the following trick: we change the sign of the odd spins and we leave unchanged the even spins, so, the Hamiltonian reads:

$$\mathcal{H} = -N\beta \sum_{\langle i,j \rangle} W(1 - \vec{\phi}_x \cdot \vec{\phi}_y). \quad (\text{A22})$$

and following the technique outlined above, we obtain the equations of the saddle point:

$$\lambda = -2W'(\rho), \quad (\text{A23})$$

$$1 - \sigma^2 = \frac{2T}{\lambda}I(m_0^2), \quad (\text{A24})$$

$$d\rho = d(1 - \sigma^2) - \frac{T}{\lambda}((2d + m_0^2)I(0) - 1), \quad (\text{A25})$$

$$\sigma(d\lambda - \mu) = 0. \quad (\text{A26})$$

Again  $m_0^2 = 2\mu/\lambda - 2d$ .

In the paramagnetic phase  $\sigma = 0$  is the solution and the equation of the critical line is (obtained by fixing  $m_0^2 = 0$ ):

$$-TI(0) = J + \frac{1}{2\sqrt{\rho_0}}, \quad (\text{A27})$$

where

$$\rho_0 = \frac{1}{2dI(0)}. \quad (\text{A28})$$

In addition  $0 < \sigma < 1$  is also a solution and so  $d\lambda = \mu$  and this implies, as in the PM/FM computation, that

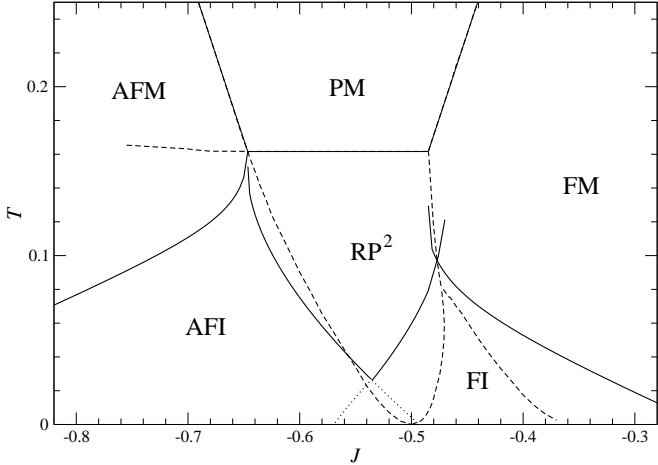


FIG. 14: Mean-Field phase diagram as obtained from the numerical minimization of the free-energy (dashed lines) and from the minimization of the free-energy calculated to fourth order (full lines). The dotted lines are artifacts of the fourth-order approximation.

$m_0^2 = 0$  The phase being a (staggered) magnetized one, this does not imply criticality. The solution is then:

$$\rho^* = \frac{1 - \sigma^2}{2I(0)d}, \quad (\text{A29})$$

and

$$T = -\frac{1 - \sigma^2}{I(0)} \left[ J + \frac{1}{2\sqrt{\rho^*}} \right]. \quad (\text{A30})$$

As in the PM-FM case, this last equation tells us what is

the magnetization  $1 - \sigma^2$  in a given point  $(T, J)$ . Again, in this part of the calculation we cannot reach the region  $J > -1/2$ . The line  $J = -1/2$  has again  $m_0^2 = 0$ .

Finally, we report the transition lines in terms of the temperature measured in the Monte-Carlo simulation. Taking into account that  $T_{\text{MC}} = T/N$ , where  $T$  is the temperature of the large  $N$  calculation and fixing  $N$  to 3, we obtain the FM-PM line:

$$T_{\text{MC}} = 1.2578 J + 0.5578, \quad (\text{A31})$$

and the AFM-PM line

$$T_{\text{MC}} = -1.2578 J - 0.793. \quad (\text{A32})$$

## APPENDIX B: MEAN FIELD FOURTH ORDER ANALYSIS

We have extended our Mean Field power expansion analysis to fourth order, so that we can find transitions where the paramagnetic phase is not involved. The analytical minimization with respect to all fields is a very hard task. But we can face the problem restricting the parameter region, using the essential fields that can describe the transition. First of all, let us explore the transitions inside the ferromagnetic region found in the second order analysis.

$$\Phi_{h\lambda_s}(\lambda_s) = \Phi(h^{\min}, 0, 0, \lambda_s), \quad (\text{B1})$$

where  $h^{\min}$  is the value of  $h$  where  $\Phi_h(h) = \Phi(h, 0, 0, 0)$  reaches the minimum. We can expand

$$\Phi_{h\lambda_s}(\lambda_s) = \Phi(h^{\min}, 0, 0, 0) + a_{h\lambda_s}(T, J)\lambda_s^2 + b_{h\lambda_s}(T, J)\lambda_s^4 + O(\lambda_s^4). \quad (\text{B2})$$

Then, if  $b_{h\lambda_s}(T, J)$  is positive there is a stable minimum with non zero  $\lambda_s$  when  $a_{h\lambda_s}(T, J)$  is negative. Therefore, we find a transition line when  $a_{h\lambda_s}(T, J) = 0$ . In this case  $b_{h\lambda_s}(T, J) > 0$  if  $T < 0.31$  and the transition line between the ferromagnetic and a ferrimagnetic phase, where  $M$  and  $M_s$  are non zero, is

$$T_{\text{FM-FI}} = -\frac{4(20 + 83\sqrt{2}J + 140J^2)}{386\sqrt{2} + 875J + \sqrt{369392 + 971810\sqrt{2}J + 1265425J^2}}. \quad (\text{B3})$$

We can do a similar analysis inside the  $\text{RP}^2$  phase. In this case we study

$$\Phi_{\lambda_s h_s}(h) = \Phi(h, 0, 0, \lambda_s^{\min}), \quad (\text{B4})$$

and

$$\Phi_{\lambda_s h_s}(h_s) = \Phi(0, h_s, 0, \lambda_s^{\min}), \quad (\text{B5})$$

obtaining the following transition lines

$$T_{\text{RP}^2-\text{FI}} = \frac{32(327 + 406\sqrt{2}J)}{35(480\sqrt{2} + 539J + \sqrt{-575136 - 768768\sqrt{2}J + 290521J^2})}, \quad (\text{B6})$$

$$T_{\text{RP}^2-\text{AFI}} = \frac{32(283 + 406\sqrt{2}J)}{35(-128\sqrt{2} + 539J - \sqrt{929312 + 1148224\sqrt{2}J + 290521J^2})}. \quad (\text{B7})$$

Finally, inside the antiferromagnetic phase we find a transition to an antiferromagnetic ordering minimizing

$$\Phi_{h_s \lambda_s}(\lambda_s) = \Phi(0, h_s^{\min}, 0, \lambda_s). \quad (\text{B8})$$

The transition line is

$$T_{\text{FM-FI}} = -\frac{4(404 + 795\sqrt{2}J + 700J^2)}{5(296\sqrt{2} + 875J + \sqrt{463688 + 1085630\sqrt{2}J + 1265425J^2})}. \quad (\text{B9})$$

The fourth-order phase-diagram is depicted in Fig. 14, together with the numerical calculation of Section. III. Letting aside the FM-RP<sup>2</sup> line (which is first-order in Mean-Field approximation), the results of the fourth-order approximation are qualitative satisfying.

---

<sup>1</sup> J. M. D. Coey, M. Viret and S. von Molnar, *Adv. in Phys.* **48**, 167 (1999).  
<sup>2</sup> See e.g. E. Dagotto, T. Hotta and A. Moreo, *Phys. Rep.* **344**, 1 (2001).  
<sup>3</sup> E. Dagotto, *Nanoscale Phase Separation and Colossal Magneto resistance*, Springer Verlag (2002).  
<sup>4</sup> J.M. Carmona et al., *Phys. Lett. B* **560**, 140 (2003).  
<sup>5</sup> See e.g., D. Amit, *Field Theory, the Renormalization Group and Critical Phenomena*, World Scientific, Singapore (1984).  
<sup>6</sup> C. Zener, *Phys. Rev.* **82**, 403 (1951); P. W. Anderson and H. Hasegawa, *ibid.* **100**, 675 (1955); P. G. de Gennes, *ibid.* **118**, 141 (1960).  
<sup>7</sup> J. A. Verges, V. Martín-Mayor and L. Brey, *Phys. Rev. Lett.* **88**, 136401 (2002).  
<sup>8</sup> J. L. Alonso, J. A. Capitán, L. A. Fernández, F. Guinea, V. Martín-Mayor, *Phys. Rev. B* **64**, 54408 (2001).  
<sup>9</sup> J. L. Alonso, L. A. Fernández, F. Guinea, V. Laliena, V. Martín-Mayor, *Phys. Rev. B* **63**, 64416 (2001).  
<sup>10</sup> J. L. Alonso, L. A. Fernández, F. Guinea, V. Laliena, V. Martín-Mayor, *Phys. Rev. B* **63**, 54411 (2001).  
<sup>11</sup> J. L. Alonso, L. A. Fernández, F. Guinea, V. Laliena, V. Martín-Mayor, *Nucl. Phys. B* **596**, 587 (2001).  
<sup>12</sup> S. Kumar and P. Majumdar, cond-mat/0305345.  
<sup>13</sup> Shan-Ho Tsai, D.P. Landau, *J. of Mag. Mat. Mag.* **226-230**, 650 (2001) 650 and *J. of App. Phys.* **87**, 5807 (2000).  
<sup>14</sup> S. Sachdev, *Quantum Phase Transitions*, Cambridge University Press, Cambridge (1999); *Science* **288**, 475 (2000).  
<sup>15</sup> J. Burgu, M. Mayr, V. Martín-Mayor, A. Moreo and E. Dagotto, *Phys. Rev. Lett.* **87**, 277202 (2001).  
<sup>16</sup> J. L. Alonso, L. A. Fernández, F. Guinea, V. Laliena and V. Martín-Mayor, *Phys. Rev. B* **66**, 104430 (2002).  
<sup>17</sup> See E. Dagotto, preprint cond-mat/0302550 and Ref. 3.  
<sup>18</sup> H. G. Ballesteros, L. A. Fernández, V. Martín-Mayor, and A. Muñoz Sudupe, *Phys. Lett. B* **78**, 207 (1996); *Nucl. Phys. B* **483**, 707 (1997).  
<sup>19</sup> S. Romano, *Int. J. of Mod. Phys. B* **8**, 3389 (1994).  
<sup>20</sup> G. Korhing and R.E. Shrock, *Nucl. Phys. B* **295**, 36 (1988).  
<sup>21</sup> S. Uhlenbruck et al., *Phys. Rev. Lett.* **82**, 185 (1999).  
<sup>22</sup> H. Nojiri, K. Kaneko, M. Motokawa, K. Hirota, Y. Endoh and K. Takahashi, *Phys. Rev. B* **60**, 4142 (1999).  
<sup>23</sup> P. Wagner, I. Gordon, S. Mangin, V.V. Moshchalkov, Y. Bruynseraede, L. Pinsard and A. Revcolevschi, *Phys. Rev. B* **61**, 529 (2000).  
<sup>24</sup> Shun-Qing Shen, R.Y. Gu, Qiang-Hua Wang, Z.D. Wang and X.C. Xie, *Phys. Rev. B* **62**, 5829 (2000).  
<sup>25</sup> P. Azaria, B. Delamotte and T. Jolicoeur, *Phys. Rev. Lett.* **64**, 3175 (1990); P. Azaria, B. Delamotte, F. Delduc and T. Jolicoeur, *Nucl. Phys. B* **408**, 485 (1993).  
<sup>26</sup> See for example H. Kawamura, *Can. J. Phys.* **79**, 1447 (2001).  
<sup>27</sup> M. Tissier, B. Delamotte and D. Mouhanna, *Phys. Rev. Lett.* **84**, 5208 (2000); M. Itakura, *J.Phys. Soc. Jpn.* **72**, 74 (2003).  
<sup>28</sup> A. Pelissetto, P. Rossi and E. Vicari, *Phys. Rev. B* **65**, 020403 (2002) and references therein.  
<sup>29</sup> B. Cooper, B. Freedman and D. Preston, *Nucl. Phys. B* **210**, 210 (1992). J.K. Kim, *Phys. Rev. Lett.* **70**, 1735 (1993). S. Caracciolo, R.G. Edwardas, A. Pelissetto and A.D. Sokal, *Nucl. Phys. B* **403**, 475 (1993).  
<sup>30</sup> See eg. G. Parisi, *Statistical Field Theory*, Addison Wesley, New York (1988).  
<sup>31</sup> P.-G. De Gennes, *Phys. Rev. Lett.* **118**, 1 (1960).  
<sup>32</sup> H. G. Ballesteros and V. Martín-Mayor, *Phys. Rev. E* **58**, 6787 (1998).  
<sup>33</sup> H. G. Ballesteros, L.A. Fernández, V. Martín-Mayor, A. Muñoz Sudupe, G. Parisi and J. J. Ruiz-Lorenzo, *J. Phys. A: Math. Gen.* **32**, 1 (1999).  
<sup>34</sup> A. M. Ferrenberg and R. H. Swendsen, *Phys. Rev. Lett.* **61**, 2635 (1988).  
<sup>35</sup> H. G. Ballesteros, L. A. Fernández, V. Martín-Mayor, A. Muñoz Sudupe, G. Parisi and J. J. Ruiz-Lorenzo, *J. Phys.*

A: Math. Gen. **32**, 1 (1999).

<sup>36</sup> M. Campostrini, M. Hasenbusch, A. Pelissetto, P. Rossi and E. Vicari, Phys. Rev. B **63**, 214503 (2001).

<sup>37</sup> M. Hasenbusch, J. Phys. A **34**, 821 (2001).

<sup>38</sup> L.A. Fernández, M.P. Lombardo, J.J. Ruiz-Lorenzo and A. Tarancón, Phys. Lett. **B277**, 485 (1992).

<sup>39</sup> A. B. Harris, J. Phys. **C7**, 1671 (1974).

<sup>40</sup> S. Caracciolo and A. Pelissetto, Phys. Rev. **E66**, 016120 (2002).

<sup>41</sup> J. Zinn-Justin, *Quantum Field Theory and Critical Phenomena*, Oxford Science Publications, Oxford (1990).